Detection of Recurrent Fluorescence Photons

Physical Review Letters (ISSN: 0031-9007)

Citation for the published paper:
Hansen, K. ; Furukawa, T. ; Matsumoto, J. et al. (2016) "Detection of Recurrent Fluorescence Photons". Physical Review Letters, vol. 117 pp. 133004.

http://dx.doi.org/10.1103/PhysRevLett.117.133004

Detection of Recurrent Fluorescence Photons

Yuta Ebara,[1] Takeshi Furukawa,[1,*] Jun Matsumoto,[2] Hajime Tanuma,[1] Toshiyuki Azuma,[3,1] Haruo Shiromaru,[2] and Klavs Hansen[4]

[1]*Department of Physics, Tokyo Metropolitan University, Hachioji, Tokyo 192-0397, Japan*
[2]*Department of Chemistry, Tokyo Metropolitan University, Hachioji, Tokyo 192-0397, Japan*
[3]*Atomic, Molecular and Optical Physics Laboratory, RIKEN, 2-1 Hirosawa, Wako, Saitama 351-0198, Japan*
[4]*Department of Physics, University of Gothenburg 41296 Gothenburg, Sweden*

(Received 10 February 2016; published 23 September 2016)

We have detected visible photons emitted from the thermally populated electronic excited state, namely recurrent fluorescence (RF), of C_6^- stored in an electrostatic ion storage ring. Clear evidence is provided to distinguish RF from normal fluorescence, based on the temporal profile of detected photons synchronized with the revolution of C_6^- in the ring, for which the time scale is far longer than the lifetime of the intact photoexcited state. The relaxation (cooling) process via RF is likely to be commonplace for isolated molecular systems and crucial to the stabilization of molecules in interstellar environments.

DOI: 10.1103/PhysRevLett.117.133004

Single molecule energy dissipation is an important issue in molecular physics and photochemistry. Internal conversion (IC), the intramolecular process by which electronic excitation energy is distributed to vibrational modes, is a common form of nonradiative transition. For the past two decades, the relaxation process of small molecules has been intensively studied by laser pump-probe experiments, and in many cases, the IC process is known to proceed on the order of picoseconds followed by prompt thermalization, i.e., statistical redistribution of the total energy into the various vibrational modes [1]. In an isolated system, inverse internal conversion (IIC) is expected to be present, whereby the transferred energy reverts to electronic excitation, followed by the emission of visible or near-infrared (IR) photons emission, referred to as recurrent fluorescence (RF). A schematic energy diagram relevant to the energy dissipation of electronic excited molecules isolated in vacuum is shown in Fig. 1. By time reversal, the IC and IIC processes are governed by the same vibronic coupling.

The thermal population of the electronic excited state is determined essentially by the ratio of the statistical weights of the respective electronic states, or equivalently, by the ratio of the rate constants of IC and IIC, namely $k_{IC}:k_{IIC}$. The sum of k_{IC} and k_{IIC}, which governs the time to equilibrium, is much higher than the radiative rate constants, and a stationary state population is therefore rapidly established after excitation. The thermally excited molecules emit two types of photons over different time scales: 1) IR photons from vibrationally excited states typically on the time scale of 100 ms and 2) visible or near-IR photons from the thermally populated electronic excited state, namely the RF, typically on the order of μs. The term of RF indicates transitions between specific electronic states. In bulk matter, the well-known phenomenon of emission of visible light in blackbody radiation is a common manifestation of the RF phenomenon. The detection of RF photons from nano and subnano particles is therefore of great interest for mapping the growth of matter from atomic to bulk scales.

The RF processes imply that generally multimode vibrational excitation, by many low energy photons or any other type of thermal excitation, can be converted into optical emission of a high energy photon, effecting a thermal pumping of optical emission. It is worth pointing out that the RF process differs from another distinct unimolecular mechanism called "thermally activated delayed fluorescence (TADF)" of organic molecules, where an excited triplet state is converted into an optically active excited singlet state via inverse intersystem crossing assisted by thermal excitation [2].

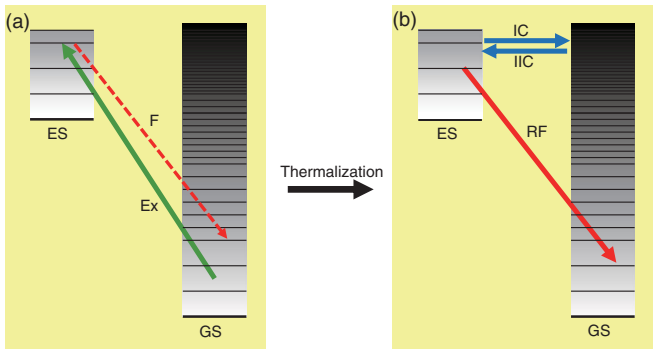

FIG. 1. Schematic energy diagram. (a) Photoexcitation followed by normal fluorescence and (b) the RF process at stationary state, respectively. The gray scale represents the vibrational level densities. GS: electronic ground state, ES: electronic excited state, Ex: photoexcitation, F: fluorescence, IC: internal conversion, IIC: inverse internal conversion, and RF: recurrent fluorescence.

The prediction and first tests of IIC and RF can be traced back to the late 1970s. Zare and co-workers reported that neutral chromyl chloride in the gas phase emits visible photons following infrared multiphoton absorption [3]. Nitzan and Jortner predicted inverse electronic relaxation, namely IIC [4]. However, because of uncertainties in the absorbed energy and the possibility of direct excitation of the electronic excited state by infrared transitions, definitive conclusions could not be made from the experiments [5].

In 1988, the RF process was theoretically revisited because of its potential importance in the evolution of interstellar molecules [6,7]. Anthracene cations, or in more general terms, polycyclic aromatic hydrocarbon (PAH) ions, are promising candidates for interstellar molecular ions. Their stability against dissociation in interstellar environment is enhanced because they can be efficiently cooled by the RF process from thermally populated low-lying electronic excited states. Carbon cluster anions C_n^- are also interesting in this context; they are expected to be present in space. In fact, C_nH^- ($n = 4, 6, 8$) have already been identified as interstellar anions [8–10]. A widely accepted mechanism of anion formation involving two-body collisions between a neutral molecule and an electron suggests that radiative cooling governs the fate of hot anions, especially for the smaller ones [11,12]. C_4^- and C_6^- also possess low-lying electronic excited states [13–15], and the fast RF cooling of these species formed by electron attachment leads to efficient stabilization by quenching the thermal electron emission.

Experimentally, the RF processes of the anthracene cations [16,17] and the small carbon cluster anions [18–21] have been recently identified, using ion storage rings and ion beam traps. These devices have enabled the study of radiative cooling processes of mass-selected and isolated molecular ions under ultrahigh vacuum conditions [22]. The measured quantity was the yield of the neutral products resulting from fragmentation or electron detachment, and the presence of RF was inferred from the suppression of this delayed unimolecular process.

Fast cooling of C_{60}^- by blackbodylike radiation was also confirmed by ion storage experiments. The delayed detachment profile indicates that radiative cooling of C_{60}^- was strongly enhanced by the presence of the surface plasmon resonance [23]. Thus, the fullerene cooling carries strong analogies to the RF process, similarly, the photons from that type of radiation have also not been detected.

In this Letter, we report the direct detection of the RF photons emitted from an isolated and mass selected molecule, with conclusive evidence that the observed photons are not ascribed to normal fluorescence nor black body emission. The source of the RF photons was hot C_6^- stored in an electrostatic ion storage ring (TMU E-ring). It has been shown previously that thermalization of the $C^2\Pi_g^+$ state is known to be very fast (of the order of picoseconds) by studying the IC process of C_6^- by laser pump-probe experiments [24]. Because the transport time from ion production to the ring is about 15 μs, the C_6^- are thermalized prior to storage.

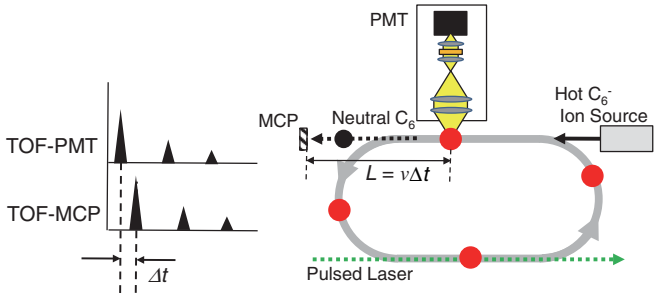

FIG. 2. Schematic layout of the experimental setup. Hot C_6^- ions were injected and stored in the TMU E-ring. The time delay (Δt) between the photon signals and the corresponding neutral product signals detected with a microchannel plate (MCP) is the time it takes for the neutral products of the velocity v to travel a distance L from the photon observation region to the position of the MCP, i.e., $\Delta t = L/v$. The Δt is constant for each ion bunch revolution. The second harmonic of a pulsed Nd:YAG laser (10 Hz, 532 nm) is merged to excite the stored ions in the opposite straight section of the ring.

The experiments are only briefly outlined while the details are given in Ref. [25] and the Supplemental Material [26]. We detected the RF photons at around 608 nm (2.04 eV) emitted from the thermally populated $C^2\Pi_g^+$ state of the C_6^- ions [14]. We employed a photomultiplier tube (PMT) combined with a bandpass filter (BPF) of 607 nm (FWHM: 70 nm) and four optical lenses, as shown schematically in Fig. 2. The typical count rate of the RF photons was limited to several counts per hour for approximately 10^5 stored ions. The temporal profile of the ion bunch was determined by the time-resolved signals from a microchannel plate (MCP) placed at the extension of the straight section of the ring, where the neutral molecules produced by collisional detachment of the ions with residual gas were detected. The size dependent revolution time was used to identify the photon source.

To examine the size specificity of the photon emission process, whether C_6^- only emits the 608 nm photons or not, the anions C_n^- ($n = 2$–6) were stored simultaneously in the ring. If all of the stored ions emitted blackbodylike photons covering a wide range of wavelengths, those photons would be always detected even under the present condition of wavelength filtering, irrespective of the species of the stored ions. On the other hand, if the stored ions emit visible photons with specific wavelengths, those photons will be blocked by the bandpass filter except for the ones from the C_6^- ions.

The temporal profile of the detected photons is shown in Fig. 3(a), wherein a series of peaks are clearly observed at the timing of the 0th, 1st, and 2nd revolutions of the C_6^- beam. The temporal profile of the detected neutrals obtained independently under the same ion storage

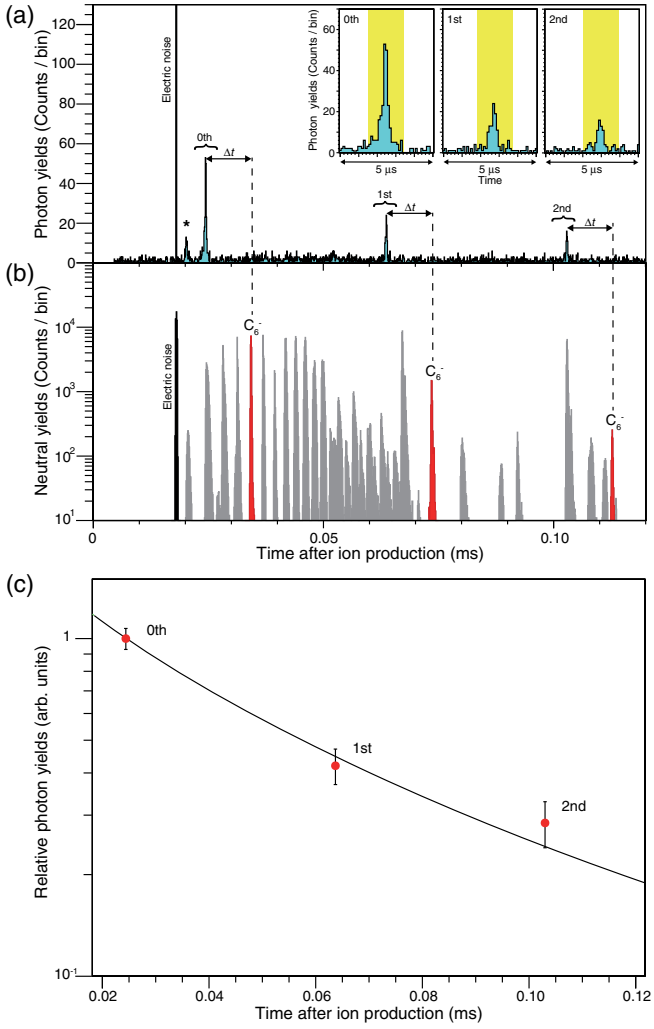

FIG. 3. RF photons from the nascent hot ions. (a) Temporal profile of the photon yield after ion production in the source. The bin width is 0.1 μs. The inset shows an expanded view of the peaks. The peak at ~ 0.02 ms, indicated by the asterisk, is unassigned. The first peak appearing just after ion injection originates from the switching noise from the injection deflector. (b) Reference temporal profile of the neutral products. The bin width is 0.1 μs. The peaks assigned to C_6^- are depicted in red. Other peaks are also assigned to C_n^- ($n \neq 6$) (see the details in the Supplemental Material [26]). Note that each peak height does not necessarily reflect the neutral intensity, because the MCP became saturated for the intense irradiation at the time before the 1st revolution of C_6^-. The time delay (Δt) between the photon signals and the corresponding neutral product signals is 9.9 μs for C_6^- (see Fig. 2). (c) Plot of time-integrated yields at the region of the ion bunch (1.9 μs in width) versus time after ion production. The error bars indicate a statistical uncertainty of $\pm 1\sigma$. The solid curves represent the simulated RF intensity assuming an initial temperature of 5000 K at the ion source. (see the Supplemental Material [26] and Ref. [19] for the details.)

conditions is shown in Fig. 3(b). During the time before the 1st revolution of C_6^-, many peaks corresponding to a range of different mass anions were observed by the neutral detector. The ions, C_n^- ($n = 2$–6), stored for a long time, periodically exhibited neutral peaks reflecting their specific m/q. However, periodic *photon* signals are only synchronized with the neutral peaks of C_6^-, which clearly demonstrates that the emitting ions are C_6^-. Thus, the time-resolved measurement enables detection of photons synchronized with the periodic passage of the C_6^- ion bunch (revolution time of 39.2 μs), which provides unambiguous proof of the origin of the RF photons.

For a more quantitative discussion, the integrated intensity over the ion bunch as a function of time after storage is compared to a simulation of the excitation energies of the ions produced in the source. The simulation takes into account the statistical electron emission and the IC and IIC processes, whose details are given in the Supplemental Material [26] and Ref. [19]. As shown in Fig. 3(c), the simulation reproduces the experimental results fairly well for a source temperature of 5000 K, which is consistent with a previous study using graphite laser ablation [28].

The RF photons were also measured as laser-induced delayed fluorescence. In this measurement, C_n^- ($n = 2$–5) were also dumped from the ring 120 μs after ion injection, and only C_6^- ions were stored in the ring. After 11.5 revolutions (approximately 0.475 ms after ion production), the second harmonic of a pulsed Nd:YAG laser was merged with the ion beam to excite the stored ions in the straight section of the ring as shown in Fig. 2. For laser irradiation, the fraction of the ions in the electronic excited states was strongly reduced compared with the nascent ions, mainly due to the limited overlap of the laser and the ion bunch.

We observed the delayed fluorescence from the stored C_6^- ions at the opposite straight section after half a revolution (19.6 μs). The configuration guaranteed that we exclusively observed ions after the completion of the IC; i.e., the observed photons were the RF photons, never normal fluorescence photons. It also ensured that only one-photon excited anions were observed, because two-photon absorption leads to fast detachment and prevents C_6^- from entering the photodetection region [19].

The measured temporal profile of the photodetection yield is shown in Fig. 4(a). The intense peak observed at the time of laser irradiation is due to scattered laser light. In addition, the background after laser irradiation was enhanced by about 80% compared with that before laser irradiation. Additional peaks were observed at 1/2 and 3/2 revolutions after laser irradiation despite the fact that they are much weaker than the scattered light. As a reference, Fig. 4(b) shows the time-resolved photon intensity observed with the countersynchronized laser, namely the laser is fired at the time the C_6^- ion bunch travels in the opposite straight section of the ring. As expected, the additional peaks are not seen. The intensities observed with the synchronized and the countersynchronized cases integrated over the corresponding ion bunch are shown in Fig. 4(c). The error bars represent a statistical uncertainty of $\pm 1\sigma$. The gray region represents the average background

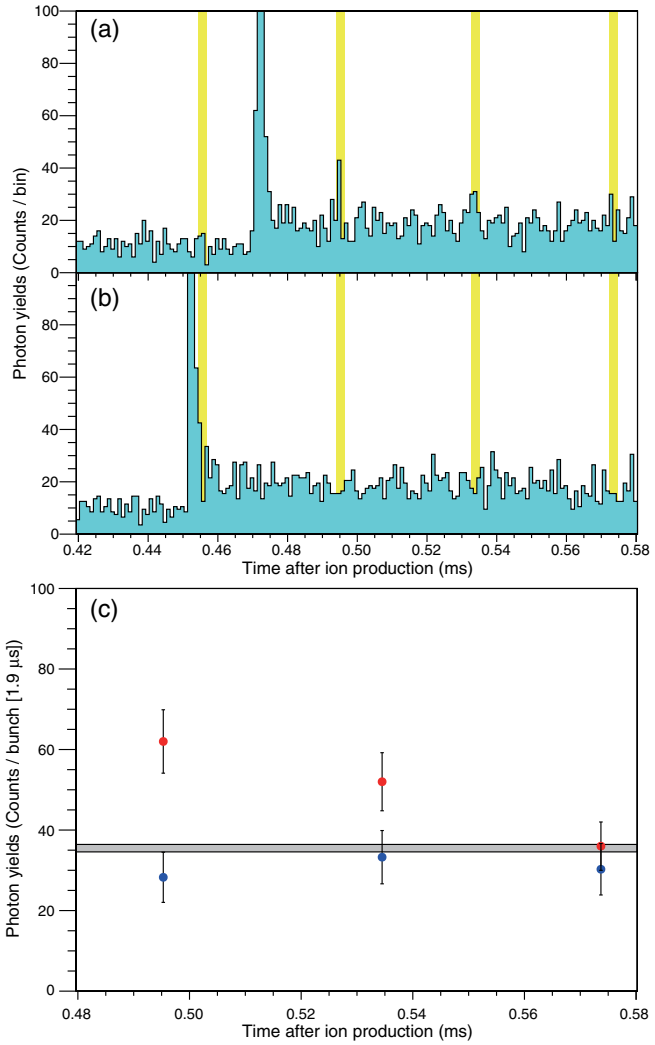

FIG. 4. RF from the photoexcited ions. (a) Temporal profile of the observed photon yield after photoexcitation (synchronized). The bin width is 1 μs. The intense peak at the time of laser irradiation (approximately 0.475 ms after ion production) is due to stray laser light. The photon emission time expected from the ion bunch timing and width (1.9 μs) are shown by the yellow regions. (b) Observed temporal photon yield after laser irradiation half a turn out of phase with the ion motion (countersynchronized). The peak position of the stray laser light shifts correspondingly by the time the ions undergo a half of a revolution. (c) Integrated yields at the ion bunch regions for both synchronized and countersynchronized cases are represented by red filled circles and blue filled circles, respectively.

yield after laser irradiation of the synchronized case with a statistical uncertainty of $\pm 1\sigma$. The treatment of the error bars are described in detail in the Supplemental Material [26]. As can be seen in the figure, enhancements in the synchronized case are statistically significant.

In conclusion, we succeeded in detecting RF photons emitted from an isolated molecule unambiguously for the first time, those from hot C_6^- produced in the source and from photoexcited C_6^-. They were identified by the time-resolved and energy-resolved information utilizing the characteristic properties of the ion storage ring. This measurement will be a milestone for the "RF photon spectroscopy" by improvement of energy resolution in the photon detection in near future.

It will give precise information to unveil the unexplored nature of the RF photons and state-selective cooling processes where the interplay of the vibrational and electronic excitation or deexcitation must be crucial. For instance, a potential application is the observation of vibrational structures both on the high- and low-energy sides of the band origin of the RF spectrum. They imply transitions from the initial vibronic state to other states accompanying the vibrational excitation or deexcitation for several modes, and provide information on the molecular structure at the instant of the RF emission, as well as on the state resolved vibronic coupling, beyond the averages generated by statistical ensembles [17].

This work was supported in part by the JSPS KAKENHI Grant No. 26220607, and by the Swedish Foundation for International Cooperation in Research and Higher Education (STINT) and the Swedish Royal Academy.

*takeshi@tmu.ac.jp

[1] V. E. Bondybey, Annu. Rev. Phys. Chem. **35**, 591 (1984).
[2] B. Valeur and M. N. Berberan-Santos, *Molecular Fluorescence: Principles and Applications* (Wiley-VCH Verlag GmbH, Weinheim, 2012), 2nd ed., p. 60.
[3] Z. Karny, A. Gupta, R. N. Zare, S. T. Lin, J. Nieman, and A. M. Ronn, Chem. Phys. **37**, 15 (1979).
[4] A. Nitzan and J. Jortner, J. Chem. Phys. **71**, 3524 (1979).
[5] J. Y. Tsao, N. Bloembergen, and I. Burak, J. Chem. Phys. **75**, 1 (1981).
[6] A. Léger, P. Boissel, and L. d'Hendecourt, Phys. Rev. Lett. **60**, 921 (1988).
[7] A. G. G. M. Tielens, Rev. Mod. Phys. **85**, 1021 (2013).
[8] M. C. McCarthy, C. A. Gottlieb, H. Gupta, and P. Thaddeus, Astrophys. J. **652**, L141 (2006).
[9] S. Brünken, H. Gupta, C. A. Gottlieb, M. C. McCarthy, and P. Thaddeus, Astrophys. J. **664**, L43 (2007).
[10] M. Agúndez, J. Cernicharo, M. Guélin, M. Gerin, M. C. McCarthy, and P. Thaddeus, Astron. Astrophys. **478**, L19 (2008).
[11] E. Herbst and Y. Osamura, Astrophys. J. **679**, 1670 (2008).
[12] R. Terzieva and E. Herbst, Int. J. Mass Spectrom. **201**, 135 (2000).
[13] P. Freivogel, M. Grutter, D. Forney, and J. P. Maier, J. Chem. Phys. **107**, 22 (1997).
[14] Y. Zhao, E. de Beer, and D. M. Neumark, J. Chem. Phys. **105**, 2575 (1996).
[15] Y. Zhao, E. de Beer, C. Xu, T. Taylor, and D. M. Neumark, J. Chem. Phys. **105**, 4905 (1996).
[16] S. Martin, J. Bernard, R. Brédy, B. Concina, C. Joblin, M. Ji, C. Ortega, and L. Chen, Phys. Rev. Lett. **110**, 063003 (2013).
[17] S. Martin, M. Ji, J. Bernard, R. Brédy, B. Concina, A. R. Allouche, C. Joblin, C. Ortega, G. Montagne, A. Cassimi,

Y. Ngono-Ravache, and L. Chen, Phys. Rev. A **92**, 053425 (2015).
[18] G. Ito, T. Furukawa, H. Tanuma, J. Matsumoto, H. Shiromaru, T. Majima, M. Goto, T. Azuma, and K. Hansen, Phys. Rev. Lett. **112**, 183001 (2014).
[19] T. Furukawa, G. Ito, M. Goto, T. Majima, H. Tanuma, J. Matsumoto, H. Shiromaru, K. Hansen, and T. Azuma, Nucl. Instrum. Methods Phys. Res., Sect. B **354**, 192 (2015).
[20] V. Chandrasekaran, B. Kafle, A. Prabhakaran, O. Heber, M. Rappaport, H. Rubinstein, D. Schwalm, Y. Toker, and D. Zajfman, J. Phys. Chem. Lett. **5**, 4078 (2014).
[21] N. Kono, T. Furukawa, H. Tanuma, J. Matsumoto, H. Shiromaru, T. Azuma, K. Najafian, M. S. Pettersson, B. Dynefors, and K. Hansen, Phys. Chem. Chem. Phys. **17**, 24732 (2015).
[22] L. H. Andersen, O. Heber, and D. Zajfman, J. Phys. B **37**, R57 (2004).
[23] J. U. Andersen C. Brink, P. Hvelplund, M. O. Larsson, B. Bech Nielsen, and H. Shen, Phys. Rev. Lett. **77**, 3991 (1996).
[24] C. Frischkorn, A. E. Bragg, A. V. Davis, R. Wester, and D. M. Neumark, J. Chem. Phys. **115**, 11185 (2001).
[25] S. Jinno, T. Takao, K. Hanada, M. Goto, K. Okuno, H. Tanuma, T. Azuma, and H. Shiromaru, Nucl. Instrum. Methods Phys. Res., Sect. A **572**, 568 (2007).
[26] See the Supplemental Material http://link.aps.org/supplemental/10.1103/PhysRevLett.117.133004, which includes Refs. [6, 13, 15, 18, 19, 25, 27], the experimental details, assignment of the peaks in the temporal profile of the neutral products, theoretical treatment on simulation of the RF decay, and the details on the RF photon data.
[27] T. Beyer and D. F. Swinehart, Commun. ACM **16**, 379 (1973).
[28] E. A. Rohlfing, J. Chem. Phys. **89**, 6103 (1988).